Session 15

Heat Transfer

CFD-based Reduced Order Model for Steel Cooling Application

[1]Oliver Scorsim ; [1]Jean-Luc Borean ;

[1]ArcelorMittal Maizieres R&D

Abstract

Thermal regulation in steel manufacturing is essential for product quality and energy efficiency. This work presents a Reduced-Order Model (ROM) for predicting steel-strip-cooling behavior along an industrial processing line. Built with Ansys' static ROM tools, it condenses the dominant thermal and flow features of high-fidelity CFD simulations into a compact surrogate that preserves key physics while sharply reducing computational cost.

To evaluate the accuracy of the ROM, additional simulations were performed using new combinations of input parameters—still within the original training bounds but not included among the training samples. The ROM closely matched the full-order simulations, reliably reproducing temperature evolution and cooling profiles for parameter combinations not used during model development.

Because the ROM delivers predictions almost instantaneously, it was integrated into a closed-loop controller capable of adjusting cooling intensity in real time. This highlights how CFD-based ROMs can retain sufficient accuracy, near CFD-like, while remaining lightweight enough for control applications.

This development fits into a framework in which the ROM can serve as a building block within a broader ecosystem of interconnected reduced-order models, potentially enabling a virtual representation of the full operation.

Keywords:

Reduced-Order Modeling (ROM)

Thermo-Fluid Dynamics

Steel Manufacturing

Real-Time Control

Cooling Process Simulation

Physics-Informed Reduced-Order Modeling for Temperature Prediction in Industrial Reheating Furnaces

[1,2]Pratibha BISWAL*; [1,2]Jetnis AVDIJAJ; [1,2,3]Alessandro PARENTE; [1,2]Axel COUSSEMENT
[1]*Aéro-thermo-mécanique (ATM), École Polytechnique de Bruxelles, Université libre de Bruxelles (ULB), Brussels, Belgium*
[2]*BRussels Institute for Thermal-fluid systems and clean Energy (BRITE), Brussels, Belgium*
[4]*WEL Research Institute, Avenue Pasteur, 6, 1300 Wavre, Belgium*

Abstract

Industrial steel reheating furnaces operate at temperatures between 800°C and 1300°C and consume a significant fraction of energy for the heating process. These units are significantly energy-intensive, and accurate prediction of furnace gas and slab temperature distributions is essential. This can help to maintain slab quality, support operational decision-making, improve thermal efficiency and enable decarbonization strategies (fuel switching, electrification). However, high-fidelity computational fluid dynamics (CFD) simulations typically require many CPU-hours per operating condition, which makes systematic design optimization impractical. In contrast, purely data-driven surrogate models can alleviate the computational cost. These methods often extrapolate poorly and can violate physics when applied outside their training envelope.

This study proposes a hybrid Reduced-Order Model with Physics-Informed Neural Network (ROM-PINN) framework for fast and physically consistent prediction of furnace and slab temperature distributions in an industrial reheating furnace. Detailed CFD simulations have been carried out and validated with real observations. These simulations are carried out for multiple syngas–natural gas blends and representative operating conditions for the industrial reheating furnace. The resulting high-dimensional CFD fields are reduced using Proper Orthogonal Decomposition (POD), yielding a compact set of dominant modes. A fully connected feed-forward neural network learns the mapping from operating parameters to the corresponding POD modal coefficients, which are used to reconstruct the full temperature field.

Radiation and conduction equations, as well as physical boundary conditions, are embedded directly into the neural network training through a multi-term loss function. The physics loss penalizes violations of Fourier heat conduction in the steel slab and radiative transfer equation (RTE) for the participating furnace gas, together with the Stefan–Boltzmann law governing the exchanges between the gas and solid surfaces and global energy conservation over the furnace control volume. An adaptive weighting strategy tracks the relative magnitudes of data and physics residuals during training.

The proposed framework can achieve speedups of several orders of magnitude compared with full CFD simulations. In addition, this model can remain robust in extrapolation which means even when applied outside the training envelope, it can avoid non-physical temperature overshooting or violating physical constraints.

Keywords: PINN, ROM, CFD, Heat transfer, Reheating furnace

Proceedings of the 1st international Symposium on AI and Fluid Mechanics
Paper No [leave blank]

Integrating Machine Learning in CFD Wall Heat Transfer Models of Impinging Jet Flows with Variable Reynolds and Prandtl Numbers

[1,2]G. Ricciardi*; [1]W. Edelbauer; [2,3]M. Gavaises; [2]B. van Wachem;

[1]*AVL List GmbH, AT*
[2]*Otto von Guericke University, DE*

[3]*City St George's, University of London, UK*

Abstract

In simulating turbulent wall bounded flows, resolving all turbulent scales down to the wall demands a significative grid refinement within the boundary layer, which becomes computationally prohibitive at high Reynolds (Re) numbers. Therefore, in computational models, wall functions are employed to express the wall shear stress and heat flux as functions of the dimensionless wall distance. Most modeling approaches for wall bounded flows still rely on equilibrium assumptions, which are often invalid, especially in complex, non-equilibrium scenarios of industrial relevance, such as impinging jets. In this context, Machine Learning (ML) techniques have attracted increasing attention to enhance traditional wall models, offering the potential to capture complex flow physics by learning dependencies directly from data, rather than relying solely on empirical or simplified physical assumptions. This work presents a data-driven wall function for turbulent impinging jet flows over a flat heated surface. The wall function is developed by using ML models, namely a Random Forest Regressor (RFR) and a Feedforward Neural Network (FNN). The general framework of standard wall functions is maintained, meanwhile an extended set of input features is incorporated to enhance the prediction of the wall heat transfer. The performance and accuracy of the RFR and FNN models are evaluated with the primary objective of assessing their capability to predict wall heat flux and temperature profiles.

Introduction

The accurate description of near wall behavior is a fundamental challenge in Computational Fluid Dynamics (CFD), particularly in turbulent regimes where accurate estimation of wall heat flux and shear stress is essential [1]. While capturing the complete velocity, temperature, and pressure gradients within the boundary layer is computationally unfeasible at high Re numbers, wall functions provide a necessary alternative by modeling near-wall transport phenomena. Within the framework of Reynolds Averaged Navier Stokes (RANS) simulations, the classic "Law of the Wall" [2] remains the most extensively used approach. However, its reliability is questionable in complex industrial flows, as the formulation was originally derived from attached flows under near equilibrium conditions. To address these limitations, Popovac et al. [3] introduced a compound wall treatment designed to incorporate non equilibrium effects, blending the integration up to the wall with the generalized wall function.

At elevated Prandtl (Pr) numbers, the thermal boundary layer is significantly thinner than the velocity boundary layer, profoundly affecting the wall heat transfer [4]. Therefore, Irrenfried et al. [5] proposed an improved P function formulation specifically for heat flux modeling at moderate Pr numbers. Šarić et al. [6] developed a two-layer formulation, named PRTL model, for high Pr number flows to better capture heat transfer and reduce mesh sensitivity. However, this approach assumes constant material properties, limiting its accuracy in industrial applications with strong temperature gradients.

In recent years, ML has been extensively integrated into CFD workflows, leveraging its capacity to generate complex, nonlinear mappings among data, to enhance current models [7]. Within the context of RANS simulations, Romanelli et al. [8] developed a wall shear stress model trained on wall-resolved RANS

*Corresponding Author, G. Ricciardi Giovanni.Ricciardi@avl.com

(WRRANS) data, while Rondeaux et al. [9] proposed a novel wall shear stress formulation for non-equilibrium flows using Direct Numerical Simulation (DNS) datasets. Despite these advancements, significantly less attention has been devoted to ML-based wall heat flux models for RANS, particularly for fluids with high Prandtl number.

In this study, a data driven model for wall heat flux prediction is developed for high Pr number impinging jet flows at varying Re number and implemented within the commercial CFD code AVL FIRE M™. To enhance the fidelity of wall heat transfer predictions, the model incorporates an extended set of input features, including pressure and temperature gradients, turbulent kinetic energy, dissipation rate, and wall shear stress. This paper is organized as follows. The *Numerical Approach* section presents the flow set up and the formulation of the data driven wall heat flux model. The *Results* section outlines the predictive performance of both approaches on two grid configurations. Finally, the conclusions of the study are discussed.

Numerical Approach

2.1 Reference Case

The dataset is based on a reference case of an impinging jet flow, analyzed across a range of Re and Pr numbers. Thermophysical properties for the Automatic Transmission Fluid (ATF) are sourced from [10]. To capture the transition from laminar to turbulent regimes, the inlet Re number varied between 1,000 < Re < 11,000, while the Pr is maintained within the 50 < Pr < 257 range. A conceptual illustration of the flow and the 2D axisymmetric computational grid used for the simulations are provided in Figures 1a and 1b, respectively.

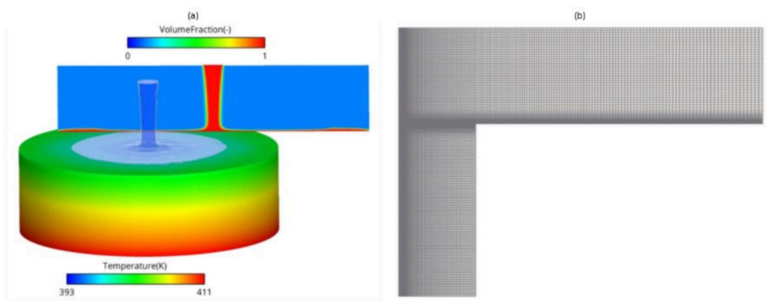

Figure 1 Flow Representation.

The RANS simulations are performed using the 3D CFD solver AVL FIRE M™ [11], which utilizes a fully conservative finite-volume discretization. Pressure-velocity coupling is managed through the SIMPLE algorithm, while first and second order accurate differencing schemes are applied to the convective terms within the transport equations. The underlying turbulence model is the approach proposed by Hanjalic et al., utilizing a low Re formulation to resolve the viscous sublayer without the use of wall functions [12]. Numerical convergence is achieved when the residuals for the momentum and turbulence transport equations fall below 10^{-5}, while the criteria is set to 10^{-6} and 10^{-4} for the energy equation and volume fraction, respectively.

Figure 2a presents the results of a mesh sensitivity analysis, while Figure 2b illustrates the validation of the heat transfer coefficient across the Re number range investigated against experimental data from [13]. The numerical results remain consistently within the 5% experimental uncertainty margin.

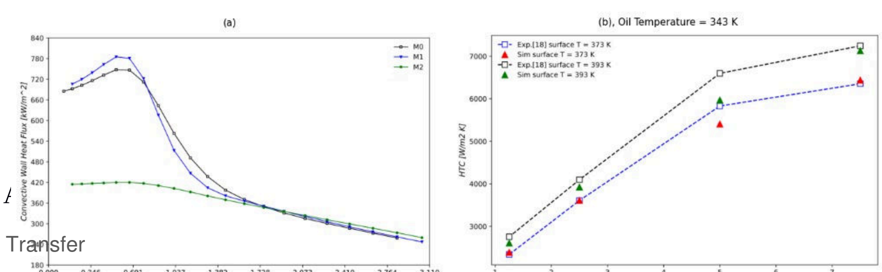

*Corresponding A

Figure 2 Mesh validation.

The converged grid is utilized to generate the dataset for the development of ML models. By leveraging exclusively WRRANS data, discrepancies within the dataset are avoided and modeling alignment between training and inference phases is ensured. On the other hand, the ML architectures inherit the same intrinsic modeling uncertainties and fidelity limitations of the turbulence model employed for closure.

The dimensionless parameters selected to characterize the flow domain are the Pr number, the Re number and the near wall Prandtl number (Pr_w). The dataset is further augmented using Sobol sampling, a quasi-Monte Carlo technique that guarantees a uniform sampling of the input space, while effectively mitigating issues related to data stratification and clustering. The input features for the ML models are extracted at cell center level from the stationary RANS fields. To ensure that the architecture encodes variable y^+ information, the volume-averaged data from a spatial stencil, comprising of up to 6 cells along the wall normal direction, are incorporated within the training set. The partitioning of the complete dataset into training, validation and testing subset, is done according to a 90/5/5 percentage split.

2.2 Data Driven Wall Heat Flux Model

The proposed ML-based wall heat flux model is founded upon the Standard Gradient Diffusion Hypothesis [14]. Analogously to the molecular heat diffusion, the model assumes a linear dependence of the turbulent heat flux on the local temperature gradient.

Equation 1. Standard Gradient Diffusion Hypothesis.

The enhanced transport properties of the turbulent flow are captured by the turbulent thermal diffusivity coefficient, according to the Prandtl analogy between momentum and heat transfer.

Equation 2. Eddy Viscosity.

In standard RANS formulations, Pr_t is treated as a constant, commonly set to 0.85. While the gradient diffusion assumption is retained in the present work, a more comprehensive set of input features is incorporated to account for complex physical phenomena often neglected in conventional wall function formulations.

Equation 3. ML based wall heat flux model.

Specifically, the local pressure gradient module , temperature gradient module , turbulent kinetic energy , eddy viscosity , wall shear stress and the near-wall Prandtl number are extracted to compute the local thermal diffusivity . These parameters are included because they critically influence the development of the thermal boundary layer and, consequently, the resulting convective heat flux.

*Corresponding Author, G. Ricciardi Giovanni.Ricciardi@avl.com

FNN and RFR are highly effective tools for mapping complex features sets to a specific target output. RFR is an ensemble leaning method, which outputs the average prediction of a multitude of decision trees. FNNs utilize a structured layer-based architecture to map an input vector to a corresponding output vector. Within each layer the data undergoes a linear transformation, followed by the application of a nonlinear activation function. The generalized mathematical formulation for the FNN is provided in Equation (4):

Equation 4. FNN architecture

$Z^{(l)}$ is the layer output, represent the input to the layer and is the nonlinear activation function. and are respectively the model weights and biases. In this study, the input and output vectors are pre-processed using standardization and min-max normalization, respectively. The ML models are developed and trained within a Python environment, employing the Scikit-learn [15] and PyTorch [16] libraries. FNN parameters are optimized by minimizing a Mean Squared Error (MSE) loss function via the *Adam* optimizer. A systematic grid search was conducted to determine the optimal hyperparameter configuration, specifically targeting the number of hidden layers, neurons per layer, and the stochastic batch size. The finalized RFR configuration consists of 100 decision trees. For the FNN, architecture comprising seven hidden layers with 64 neurons per layer is selected to balance predictive accuracy and training time. Activation functions, including ReLU and Tanh, are implemented to handle the nonlinear nature of the flow data. The learning curves for the FNN are provided in Figure 3, while a comparative performance analysis across the training, validation, and testing subsets is detailed in Table 1.

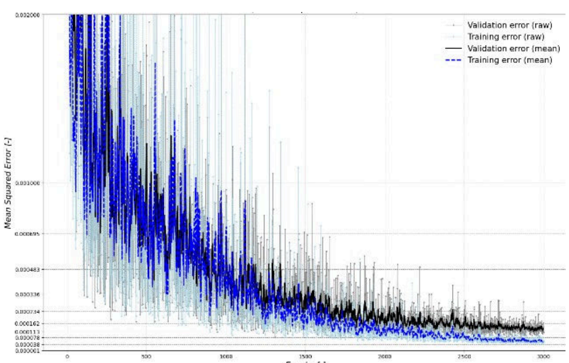

Figure 3. FNN training and validation curves.

Table 1. Training, validation and testing MSE for the ML models

Results

	Training [MSE]	Validation [MSE]	Testing [MSE]
FNN	**$5.4x\ 10^{-5}$**	**$1.0x\ 10^{-4}$**	**$1.1x\ 10^{-4}$**
RFR	**$6.13x\ 10^{-5}$**	**$4.74x\ 10^{-4}$**	**$3.13x\ 10^{-4}$**

*Corresponding Author, G. Ricciardi Giovanni.Ricciardi@avl.com

To evaluate the performance of the ML-based wall functions a posteriori, the trained models are integrated into the industrial CFD solver AVL FIRE M™. The models are benchmarked against four unseen test cases, combining two Re numbers (Re = 4000, 8000) with varying bulk and near-wall Pr numbers (Pr = 250, 190

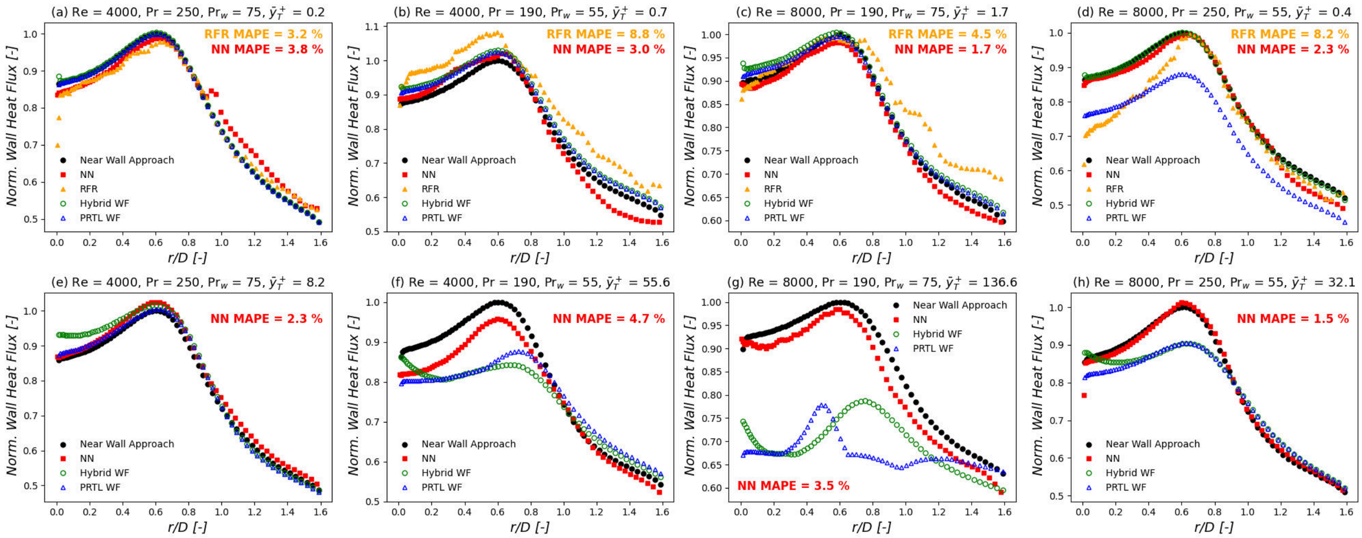

Pr_w= 75, 55). To investigate the influence of the mesh on model accuracy, each case is simulated using both a refined and a coarsened grid architecture. The Mean Absolute Percentage Error (MAPE) is employed as the primary metric for performance comparison between the ML based wall heat flux models, the PRTL model and the hybrid wall formulations [11]. The outcomes are reported in Figure 4.

Figure 4 Comparative analysis of the wall heat flux predictions using ML-based formulations, the PRTL model, and the hybrid wall function. Panels (a)–(d) represent the fine mesh configuration, while panels (e)–(h) correspond to the coarse grid results.

For the fine mesh configurations, where the thermal wall unit y^+_T remained below 2, both the RFR and the FNN exhibit high fidelity, consistent with the high-resolution data used during the training phase. As illustrated in Figure 4 (a) through (d), both ML architectures demonstrate comparable accuracy to the near wall approach, effectively replicating wall resolved data. However, the FNN consistently yields lower MAPE than both the RFR and the two wall models. A critical test is conducted by increasing the near-wall cell size by a factor of three, resulting in an almost tenfold increase in the average y^+_T. Under these coarser conditions, the RFR proves unstable. Conversely, the FNN architecture demonstrates robustness, maintaining a much more limited mesh dependency compared to all other tested formulations. Specifically, case (g) highlights a regime where the FNN provides a physically consistent heat flux description even as the thermal y^+_T exceeds 100. In contrast, both the PRTL and Hybrid wall functions exhibit a significant, mesh-dependent degradation in predicted heat transfer.

Conclusion

The current study proposes a ML-based wall heat flux model tailored for impinging jet flows characterized by variable Re and Pr numbers. The model, which has been rigorously validated against both experimental and numerical data, represents a novel approach to modeling the thermal boundary layer at high Pr numbers using ML techniques and leveraging a dataset derived from WRRANS simulations. The computational cost associated with the inference phase is negligible compared to the simulation turnaround time. Implementation of this model across variable mesh resolutions demonstrates a significant capacity to mitigate mesh dependency when compared to the PRTL model and the hybrid wall modeling. The results indicate a substantial improvement in predictive accuracy, alongside the potential to maintain

*Corresponding Author, G. Ricciardi Giovanni.Ricciardi@avl.com

computational reliability on meshes up to three times coarser than those traditionally required. Nevertheless, the model exhibits limitations regarding its generalization capabilities, particularly in regimes where near-wall behavior is poorly resolved. Future research will focus on extending the model's applicability to a broader range of flow categories to enhance its robustness and generalizability.

Acknowledgments

Financial support from the HORIZON-MSCA-2022-DN-01 program, under REA grant agreement n. 101120014 is acknowledged.

References

1. B.E. Launder, D.B. Spalding (1974). *The numerical computation of turbulent flows*. Computer Methods in Applied Mechanics and Engineering, 3(2):269-289.

2. D. C. Wilcox (2006). *Turbulence Modeling for CFD*, 3rd ed. La Cañada, CA: DCW Industries.

3. M. Popovac, K. Hanjalic (2007). *Compound Wall Treatment for RANS Computation of Complex Turbulent Flows and Heat Transfer*. Flow Turbulence Combust, 78:177–202.

4. C. Irrenfried (2020). *Convective turbulent near wall heat transfer at high Prandtl numbers: A modelling approach based on Direct Numerical Simulations and experiments.* M. B. Lesser.

5. C. Irrenfried and H. Steiner (2017). *DNS based analytical P-function model for RANS with heat transfer at high Prandtl numbers*. Int. J. Heat and Fluid Flow, 10:217-225.

6. S. Šarić, and B. Basara (2018). *A near-wall model for heat transfer at high Prandtl numbers*. Tenth International Conference Computational Fluid Dynamics, Barcelona, Spain, July 9-13, 2018.

7. R. Vinuesa and S. L. Brunton (2022). *Enhancing computational fluid dynamics with machine learning*. Nature Computational Science, 2(6): 358–366.

8. M. Romanelli, S. Beneddine, I. Mary, H. Beaugendre, M. Bergmann, D. Sipp (2023). *Data-driven wall models for Reynolds Averaged Navier–Stokes simulations.* International Journal of Heat and Fluid Flow, 99.

9. E. Rondeaux, A. Poubeau, C. Angelberger, M. Munoz Zuniga, D. Aubagnac-Karkar, and R. Paoli (2024). *Exploring the potential and practical usability of a machine learning approach for improving wall friction predictions of RANS wall functions in non-equilibrium turbulent flows*. Flow, Turbulence and Combustion, 112(4): 975–1000.

10. A. Poubeau, G. Vinay, B. Kekelia, K. Bennion (2023). *Numerical simulations of high Prandtl number liquid jets impinging on a flat plate*. International Journal of Heat and Mass Transfer, 205.

11. AVL List GmbH. (2026). *AVL FIRE™ M v2026.1 User Manual*. Graz, Austria: AVL List GmbH.

12. K. Hanjalic, M. Popovac, and H. Hadziabdic (2004). *A Robust Near-Wall Elliptic-Relaxation Eddy-Viscosity Turbulence Model for CFD*. International Journal of Heat and Fluid Flow, 25:1048-1051.

13. B. Kekelia, K. Bennion, X. Feng, G. Moreno, J. E. Cousineau, S. Naru-manchi, J. Tomerlin, (2019). *Surface Temperature Effect on Convective HeatTransfer Coefficients for Jet Impingement Cooling of Electric Machines With Automatic Transmission Fluid*, ASME 2019 International Technical Conference and Exhibition on Packaging and Integration of Electronic and Photonic Microsystems, California

14. S. B. Pope, (2000). *Turbulent Flows*. Cambridge University Press.

*Corresponding Author, G. Ricciardi Giovanni.Ricciardi@avl.com

15. F. Pedregosa, G. Varoquaux, A. Gramfort, V. Michel, B. Thirion, O. Grisel, M. Blondel, P. Prettenhofer, R. Weiss, V. Dubourg, J. Vanderplas, A. Passos, D. Cournapeau, M. Brucher, M. Perrot, and E. Duchesnay (2011). *Scikit Learn: Machine Learning in Python*, J. Mach. Learn., 12:2825–2830

16. A. Paszke, S. Gross, F. Massa, A. Lerer, J. Bradbury, G. Chanan, and S. Chintala (2019). *PyTorch: An imperative style, high-performance deep learning library.* Advances in Neural Information Processing Systems, 32:8024-8035.

*Corresponding Author, G. Ricciardi Giovanni.Ricciardi@avl.com

A Machine Learning wall function for heat transfer prediction in laminar flows at high Prandtl number

Rémy Souan*[1], Adèle Poubeau[1], Thibault Fanney[1], Lionel Mathelin[2], Anne Sergent[2,3], and Christian Angelberger[1]

[1]IFP Energies nouvelles, 1–4 Av. du Bois Préau, 92852 Rueil-Malmaison, France
[2]Laboratoire Interdisciplinaire des Sciences du Numérique (LISN), CNRS, Université Paris-Saclay, Orsay, 91400, France
[3]Sorbonne Université, Faculté des Sciences et Ingénierie, UFR Ingénierie, Paris, 75005, France

Abstract

The increasing demand for compact and high-performance electric motors in sustainable transportation systems leads to strong thermal constraints, making efficient cooling strategies essential. Accurate prediction of liquid–solid heat transfer is therefore a key challenge, particularly when using oil as a coolant, characterized by high Prandtl numbers ($100 < Pr < 400$). In such conditions, thermal boundary layers are significantly thinner than hydrodynamic ones, requiring very fine near-wall meshes in high-fidelity simulations and resulting in prohibitive computational costs.

Thermal wall functions (WF) provide a cost-effective alternative but rely on restrictive assumptions, limiting their applicability to simple flow configurations. In this work, a Machine Learning Wall Function (MLWF) is proposed to overcome these limitations and extend modelling capabilities to more complex flows.

The proposed approach aims to learn the relationship between wall heat flux and near-wall flow variables from fully resolved simulations. To evaluate the MLWF method, the study first focuses on heated flat-plate simulations, while more complex configurations involving recirculation zones will be investigated in future work. This setup allows direct comparison between the MLWF and thermal WF predictions. A Kolmogorov–Arnold Network (KAN) is used because it can perform symbolic regression and provide an explicit analytical formulation. This is important since the resulting expression is implemented directly as a WF in CFD solvers, without introducing any additional computational cost which may be associated with neural network based models.

Preliminary results demonstrate that the MLWF well predicts wall heat flux while reducing computational cost compared to fully resolved simulations. Its robustness is further assessed across varying Reynolds numbers, showing promising generalization capabilities.

Keywords: Machine learning; Thermal wall law; Laminar flow; Oil cooling.

*Corresponding author

1 Introduction and Context

The rapid development of electric vehicles has led to increasingly compact electric machines, resulting in higher thermal loads and stricter cooling requirements. Efficient thermal management is therefore a key challenge to ensure performance, reliability, and durability of these systems. Advanced direct liquid cooling strategies, often based on oil as a coolant, are currently investigated due to their high heat removal and dielectric capabilities.

However, oil is characterized by a high Prandtl number, which leads to the formation of two different scales: the very thin thermal scale (0.1 mm) compared to the hydrodynamic one (1 mm). As a result, numerical simulations aiming at accurately predicting heat transfer must resolve very fine thermal boundary layers near the wall. This induces prohibitive computational costs, especially in three-dimensional configurations relevant for industrial applications [2].

To overcome this limitation, modelling strategies known as thermal WF have been developed [1]. This approach assumes a self-similar near-wall temperature profile to predict the wall heat flux with first near-wall cell flow variables, without resolving the thermal boundary layer. WF significantly reduces the computational cost. Nevertheless, their applicability remains limited to simplified flow configurations.

Thermal WF rely on strong assumptions regarding the structure of the near-wall flow. In particular, they typically assume: negligible wall-normal velocity and flat plate. These assumptions are often satisfied in canonical configurations such as laminar boundary layers over an heated flat plate, but they break down in more complex flows involving separation, curvature, or recirculation. In such cases, the near-wall velocity field is no longer purely tangential, and the thermal boundary layer structure deviates from the theory. For instance, in flows over a two-dimensional hill geometry, an adverse pressure gradient induces flow separation and recirculation. In these regions, the wall-normal velocity component becomes non-negligible, violating the hypotheses underlying classical WF. Consequently, WF predictions lead to large discrepancies between analytical and numerical results.

These limitations highlight the need for alternative modelling strategies capable of capturing complex near-wall physics without relying on restrictive assumptions. A machine learning (ML) based approach is proposed to overcome these issues, with a particular focus on Kolmogorov–Arnold Networks (KAN). KANs have been shown to achieve prediction accuracy comparable to conventional NN [3], while enabling symbolic regression to extract an explicit analytical formulation. This is an additional step of the KAN training. This capability is especially valuable for scientific machine learning applications, as it provides models that can be efficiently integrated into CFD solvers while avoiding any additional computational time typically associated with KAN or NN approaches.

The KAN based symbolic regression model is trained using high-fidelity simulations in which the temperature field is fully resolved, allowing the network to learn the relationship between near-wall flow quantities and wall heat flux. Once trained, the resulting model is intended to be implemented as a WF in CFD under-resolved simulations.

2 Methodology

The methodology presented here is assessed with the heated flat-plate case. The same framework is intended to be extended in future work to more complex configurations involving separation and recirculation effects.

This work proposes a Machine Learning Wall Function (MLWF) based on a KAN architecture combined with symbolic regression. The objective of the MLWF is to learn a mapping function $\mathcal{F}$ between near-wall flow quantities and wall heat flux from fully-resolved simulations, which is for the heated flat plate configuration:

$$q_w = \mathcal{F}(y, \tilde{u}, \tilde{T}), \tag{1}$$

where y is the wall distance, $\tilde{u}$ and $\tilde{T}$ are filtered velocity. This model is then implemented in a CFD solver to predict the wall heat flux in heated flat plate coarse simulations.

The learning workflow consists of four main steps:

- Construct a database from fully resolved simulations of a heated flat plate with a linear inlet velocity profile with various flow configuration. The training dataset is built by extracting input–output pairs associating near-wall flow variables inside the thermal boundary layer with the corresponding wall heat flux. This step is crucial as the diversity of this database largely determines the range of applicability of the resulting MLWF.
- Select and filter fully-resolved flow variables to be used during training. The filtering procedure ensures that the inputs used during MLWF training are consistent with flow variables available during deployment in a coarse simulation.
- Train the MLWF model. In this work, we choose a KAN (Kolmogorov Arnold Network) as it allows a post training symbolic regression step that facilitates the integration into the CFD solver CONVERGE.
- Test the MLWF on under-resolved CFD simulations (heated flat plate numerical setup). This involves integrating the learned MLWF model (KAN-based symbolic regression formula) in CONVERGE.

3 Results

The MLWF is first validated on the heated flat plate configuration with a linear inlet velocity profile at $Re = 360$. Low fidelity simulations (LF) without wall modeling (referenced as $q_w^{LF} Re = 360$ on Figure. 1a) strongly underestimate heat transfer compare to high-fidelity simulations (HF) (referenced as $q_w^{HF} Re = 360$ on Figure. 1a), the MLWF ($q_w^{MLWF} Re = 360$) well reconstructs both the magnitude and spatial evolution of the wall heat flux when tested on this LF simulation configuration (see Figure. 1a). In particular, the MLWF starts from an initial state at rest and converge as quickly as the WF approach towards the final state. Indeed, the KAN based symbolic regression formula is trained with a dataset built by extracting input–output pairs from several time steps, including both transient and steady regimes. This procedure is repeated for each flow configuration (Reynolds number). This allows the MLWF to predict correctly the wall heat flux at each time step of the CFD solver for various flow conditions.

The generalization capability of the MLWF is evaluated by training and validating the model on various Reynolds number of the heated flat plate numerical setup: 180, 240, 300, 360, and 420 (only the MLWF predictions for 360 and 420 referenced as $q_w^{MLWF} Re = 360$ and $q_w^{MLWF} Re = 420$ are shown on Figure. 1a) and then only testing on 480, 700, 900 (referenced as $q_w^{MLWF} Re = 480$, $q_w^{MLWF} Re = 700$ and $q_w^{MLWF} Re = 900$ on Figure. 1a).

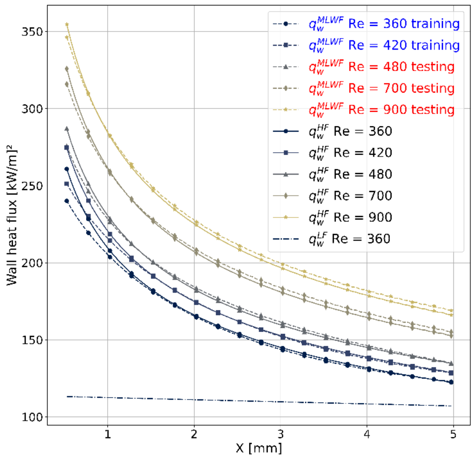

(a) MLWF wall heat flux prediction results (q_w^{MLWF}) on the heated flat plate at Reynolds 360, 420, 480, 700 and 900. Reynolds configurations at 360 and 420 in blue are seen during training, while 480, 700 and 900 in red are only for testing the MLWF extrapolation capabilities. MLWF predictions are compared to the high fidelity results (q_w^{HF}) for Reynolds numbers: 360, 420, 480, 700 and 900

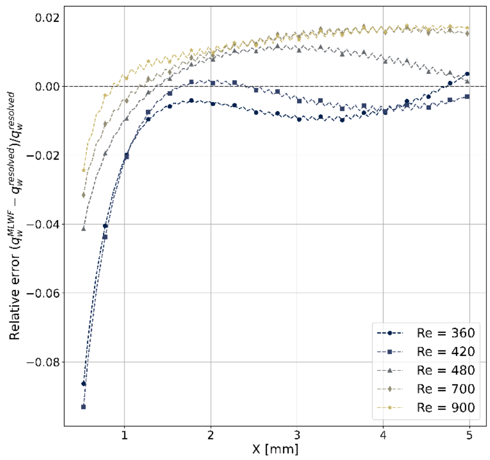

(b) q_w^{MLWF} relative error on the heated flat plate at Reynolds 360, 420, 480, 700 and 900.

The results show that the MLWF maintains good predictive performance across different Reynolds numbers and therefore extrapolating well, (see Figure. 1a). Most predictions falling within a ±2.5% error range (see Figure. 1b). The main error peak is observed near the inlet, where the thermal boundary layer starts its development and is extremely thin. HF simulations are poorly resolved in this zone and these data are not included in the training database. So the MLWF is extrapolating, that is why the error is higher in this zone.

Despite promising results and efficient implementation in CONVERGE, the symbolic regression formula obtained with KAN leads to complex and non-interpretable analytical expressions. Moreover, robust generalization may require large training datasets covering a wide range of additional flow conditions, such as variations in Prandtl number, wall temperature, and flow configuration like recirculation, which can significantly increase the computational cost associated with generating high-fidelity simulations. These limitations highlight the intrinsic difficulty of purely data-driven approaches and motivate future developments toward hybrid modelling strategies using both WF and MLWF.

4 Conclusion

This work demonstrates the feasibility of building a MLWF for high-Prandtl laminar flows using a KAN-based symbolic regression framework. The proposed approach well predicts wall heat flux in under-resolved simulations for the simple case of a flow over a flat plate. However, challenges remain in terms of generalization, and applicability to complex flows. Future work will focus on extending the MLWF to more complex configurations including flow with recirculation zones.

References

[1] Adrien Ingles. "A Near-Wall Model for Heat Transfer Prediction in Laminar Flows at High Prandtl Number: Application to Impinging Liquid Jets for Electric Motor Cooling". PhD thesis. IFPEN: Montpellier, Feb. 19, 2026. 203 pp.

[2] Adèle Poubeau et al. "Numerical simulations of direct liquid cooling of the end-windings of an electric machine". In: *International Journal of Heat and Mass Transfer* 235 (Dec. 2024), p. 126162. ISSN: 00179310. DOI: `10.1016/j.ijheatmasstransfer.2024.126162`. URL: `https://linkinghub.elsevier.com/retrieve/pii/S001793102400992X` (visited on 05/12/2025).

[3] Runpeng Yu, Weihao Yu, and Xinchao Wang. *KAN or MLP: A Fairer Comparison.* Aug. 17, 2024. DOI: `10.48550/arXiv.2407.16674`. arXiv: `2407.16674[cs]`. URL: `http://arxiv.org/abs/2407.16674` (visited on 02/07/2026).

Proceedings of the 2nd international Symposium on AI and Fluid Mechanics
Paper No [leave blank]

Reconstructing Boiling Heat Transfer and Inferring Near-Wall Hydrodynamics from High-Resolution Optical Diagnostics and Optical Flow of Nucleate Boiling

[1]Matthew T. Hughes; [2]Christos Markides; [3]Matteo Bucci*;

[1]*Department of Mechanical Engineering, University of Michigan, Ann Arbor, MI 48109, USA*

[2]*Clean Energy Processes (CEP) Laboratory, Department of Chemical Engineering, Imperial College London, London, SW7 2AZ, UK*

[3]*Department of Nuclear Science and Engineering, Massachusetts Institute of Technology, Cambridge, MA 02139, USA*

Keywords: Boiling; CNN; Experimental data; Optical flow

Abstract. Reconstructing boiling heat transfer from optical images has gained significant attention in recent years but achieving highly accurate and generalizable models remains challenging. One major limitation is the lack of near-wall hydrodynamic measurement data, as bubbles can substantially alter the size and development of the thermal boundary layer. If the near-wall hydrodynamics can be inferred directly from optical images, then a more physically consistent and accurate reconstruction of boiling heat transfer may be feasible. In this work, we leverage our existing database of high-resolution optical diagnostics of boiling heat transfer, which includes synchronous liquid-vapor phase detection images and wall temperature and heat flux distributions measured via infrared thermometry. We take the liquid-vapor phase detection videos alone and perform optical flow on these images to estimate the changes in near-wall hydrodynamics from bubble nucleation, growth, and departure. We also track the local time a region of the boiling surface has been wet to estimate the baseline transient conduction liquid heat transfer coefficient. The corresponding wall temperature and heat flux measurements are stored separately and used as training, testing, and validation data. The resulting velocity fields and wet time distributions are then provided to a convolutional neural network to obtain high-resolution heat transfer coefficient measurements in the liquid phase. Predictions are validated against independent infrared thermometry measurements, demonstrating improved accuracy and physical consistency. The results establish a pathway for extracting near-wall transport information from optical data alone and provide guidance for future measurement and preprocessing strategies.

1. Introduction

Accurate prediction of boiling heat transfer is essential for the safe and efficient operation of high-heat-flux energy and thermal management systems. Despite decades of research, physically consistent models of nucleate boiling remain limited in their predictive capability. One of the most widely adopted modelling frameworks is heat flux partitioning (HFP), which decomposes the total wall heat flux into contributions from forced convection, transient conduction, and evaporation [1]. While HFP is grounded in physical mechanisms, its constituent models largely rely on analytical or empirical descriptions derived from simplified or isolated experiments, neglecting collective effects arising from liquid-vapor interactions during boiling. Prediction error of individual heat transfer mechanisms that are on the order of 100% have been reported [2,3], even if the average heat transfer rate predictions are within 20% of measurements. This suggests that HFP is still not yet a predictive model of "unit-cell" heat transfer mechanisms, and a more precise understanding of the collective effects during boiling heat transfer is necessary. A recent study by Aguiar et al. [4] provides new evidence for a missing physical mechanism during boiling. The study employed multi-modal, high-resolution diagnostics to directly measure time- and space-resolved single-phase liquid heat transfer coefficients (HTC) during subcooled flow boiling. These measurements revealed that the liquid HTC evolves from a transient-conduction-dominated regime toward a steady-state value. Crucially, they found that the presence of bubbles enhances both the transient and steady-state single-phase HTC. In fact, the steady-state HTC can increase by a factor of five as the critical heat flux limit is approached, a magnitude of enhancement that is simply not captured by current HFP models. Typically, HFP models transient conduction using one-dimensional analytical solutions and models forced convection in similarly simplified manner by assuming bubbles effect as if they created a rougher surface. To address this missing mechanism, Aguiar et al. [4] proposed that the effective shear velocity, and consequently the effective thermal conductivity, has been enhanced by the momentum imparted by growing vapor bubbles. While the results clearly show a strong correlation between momentum added by bubbles and heat transfer enhancement, a simple and accurate description of this mechanism remains elusive. If the effective thermal diffusivity enhancement produced by bubbles can be accurately quantified by optical images alone, it may be possible to reconstruct boiling heat transfer across a wide variety of operating conditions and working fluids. In this work, we investigate the potential of optical flow to measure the agitation of the liquid by bubbles. Optical flow is the pattern of apparent motion of edges in a scene caused by the relative motion between an observer and the scene.

2. Overview of experiment and advanced diagnostics

The experimental data consists of steady-state subcooled flow boiling of water at 1.21 bar. The mass flux ranges from 500 to 1500 kg m^{-2} s^{-1}, and the degree of subcooling ranges from 10 to 20 K. The channel is a 30 mm × 10 mm rectangle, where one side of the channel is heated using a conductive thin-film coating of indium tin oxide (ITO). ITO is an optically transparent and infrared opaque material, enabling optical access of the boiling process and infrared imaging of the heated wall. The ITO is coated on a 10 mm × 10 mm region of a sapphire substrate that is 20 mm × 20 mm × 1 mm.

The optical diagnostics and test section are shown in Fig. 1. The optical diagnostics include one high-speed video camera and one high-speed infrared camera. Both cameras image the back of the boiling surface. The high-speed video camera is placed at a slight angle to perform a technique known has phase-detection [5]. This technique allows us to discern the microlayer, liquid, and dry regions of the boiling surface. The infrared camera records radiation emitted from the ITO, sapphire substrate, and background, which yields instantaneous measurements of the wall temperature across the heated area using a calibration technique by Bucci et al [6]. This procedure involves solving the heat diffusion equation within the sapphire substrate, which in turns yields the local heat flux to water. The combination of local wall temperature and heat flux measurements allows the direct calculation of the local heat transfer coefficient. During our experiments, we record the infrared and phase detection images synchronously, allowing us to align the videos spatially and temporally. This way, the two sets of images can be overlapped, enabling a measurement technique that can isolate heat removed by single-phase liquid heat transfer, microlayer evaporation, and single-phase vapour heat transfer. For this work, we focus on the single-phase liquid heat transfer, since that is typically where most of the heat is removed during boiling [2,4].

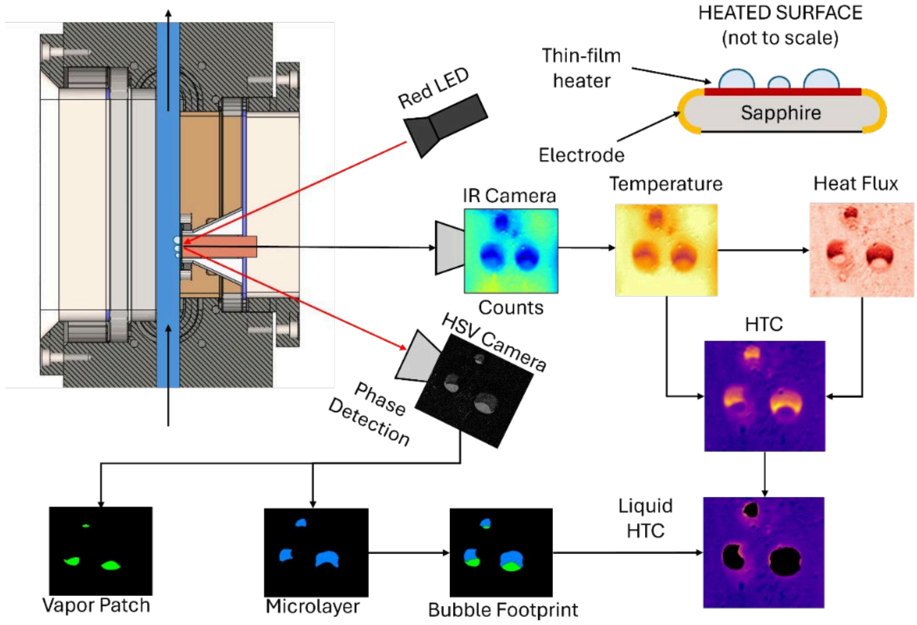

Figure 1. Experimental test section and overview of optical diagnostics. Obtained from Aguiar et al. [4].

3. Machine learning model development

The first input feature is the velocity field generated from optical flow of our phase detection videos. In this case, we use the Farneback algorithm, which estimates motion based on polynomial expansion. The second input feature is also derived from our phase detection images. Precisely, the second input feature represents the local single-phase heat transfer coefficient based on one-dimensional transient conduction. The local, instantaneous transient conduction heat transfer coefficient is calculated in advanced using the following equation:

where is the effusivity of the liquid, is the steady-state forced convection heat transfer coefficient in the absence of bubbles, and is the local, instantaneous time a pixel has been wet. An example of these input features is shown in Fig. 2. It should be noted that the heat transfer coefficient given by Equation 1 has been shown to systematically underpredict the local, instantaneous heat transfer coefficient. By including an estimate of the near-wall fluid motion, provided from optical flow, it may be possible to account for convective heat transfer enhancement due to the presence of bubbles.

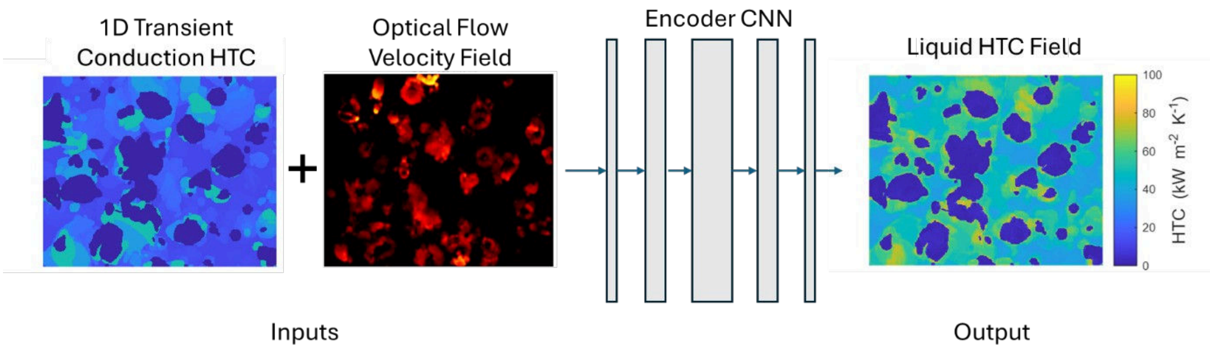

Figure 2. CNN model architecture. The inputs are the liquid heat transfer coefficient calculated from a 1D mechanistic reconstruction, and the magnitude of the velocity field as measured by our optical flow processing. The output is the liquid heat transfer coefficient field, which we compare against our experimental infrared thermometry measurements.

To that end, a convolutional neural network (CNN) is used to predict the liquid HTC field. Briefly, CNNs are a class of deep feedforward neural network that extracts local features of an image by performing convolutions on the input features with a fixed number of kernels at a predefined size. The schematic of the CNN network, its input features, and output features are shown in Fig. 2. The input features consist of the velocity fields obtained from optical flow, and the 1D mechanistic liquid heat transfer coefficient field. Since the spatio-temporal trends in the liquid-heat transfer coefficient are well-captured by the mechanistic reconstruction, a relatively simple CNN network is used. The model is trained using ~70% of the experimental dataset, where specific cases are omitted and used as validation data. The model is trained using 100 epochs and an adaptive learning rate starting at 0.001. It should be noted that the input features and output features are scaled by the minimum and maximum values of the training data so that the range of the numerical values for the validation and training data approximately falls in the range of [0, 1].

4. Sample results and discussion

First, the relationship between the enhanced steady-state liquid HTC and average velocity magnitude measured by optical flow is demonstrated in Fig. 3. One can observe that the magnitude of the steady-state HTC (i.e., the HTC in regions of the heating surface that have remain wetted for sufficiently long time) increases with the square root of the average velocity. It was previously observed that an increasing shear velocity may explain the observed enhancement in the transient and steady-state HTC that make up the overall liquid HTC. These results also suggest that the momentum generated by bubbles may influence the enhancement of the liquid HTC.

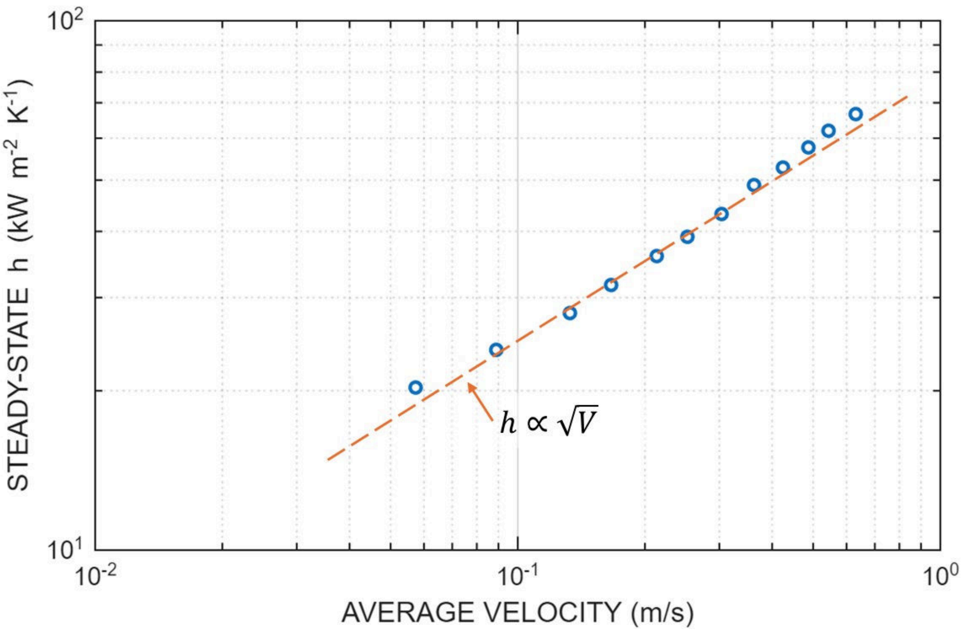

Figure 3. The steady-state liquid heat transfer coefficient versus the average magnitude of the velocity field measured by our optical flow image processing.

Fig. 4 shows how the velocity field changes near a growing bubble. Once a bubble nucleates, the intensity of the image increases, leading to a vector field nominally pointing radially outward, with a magnitude that is related to the rate the dry spot and microlayer grow. As the overall bubble footprint size reaches its apex, the magnitude of the velocity field decreases. Once bubble departure takes place, the velocity field magnitude starts to increase again, with the direction of the flow being radially inward. These measurements provide an indication of the near-wall velocity fluctuations during bubble growth and departure and provide a more quantitative measure of the momentum imparted by boiling, potentially explaining why the effective thermal diffusion is enhanced.

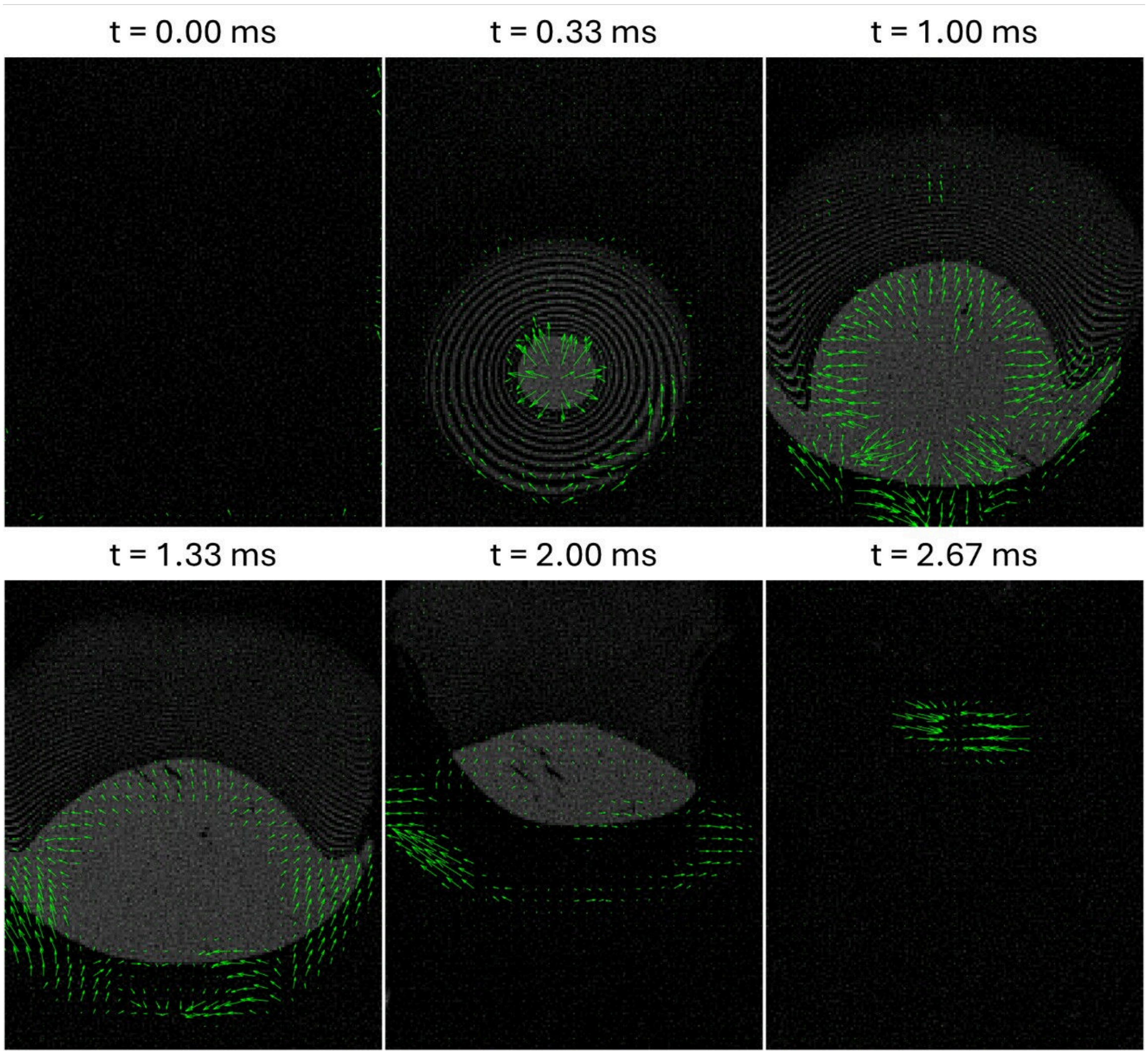

Figure 4. Timelapse of the optical flow field around a vapour bubble.

Fig. 5 shows the ability of the CNN to predict the local, instantaneous HTC. We also show the 1D transient conduction reconstruction to show the difference between the purely mechanistic reconstruction and CNN reconstruction. It can be seen that the predictive accuracy of the CNN greatly exceeds the 1D mechanistic reconstruction. Across all cases, the average root-mean-square error is 9%. In general, it can be seen that the liquid HTC near bubbles is larger than the liquid HTC in the "far-field" region, consistent with our experimental measurements. Additionally, one can observe that the far-field liquid HTC in the case of the CNN yields values far larger than the steady-state forced convection HTC. These preliminary results clearly demonstrate that the CNN can at least account for some of the main observations from experimental infrared imaging of boiling. However, the CNN still does not yield perfect agreement with the measurements. In Fig. 5, one can observe that the CNN can severely over-predict and under-predict the liquid HTC in a few locations. This is likely because the instantaneous velocity field in the model may be interpreted as a quasi-local enhancement in thermal diffusion; however, our experimental observations indicate that the far-field HTC increase is essentially uniform across the heating surface. It may be beneficial to treat near-wall velocity fluctuations as a more global feature of the image. CNN architectures with larger receptive fields, such as deeper networks, larger convolution kernels, dilated convolutions, or encoder-decoder architectures, may better capture this behaviour. Alternatively, the 1D transient conduction reconstruction could be simply scaled by the magnitude of the optical velocity field as it compares to the momentum of the bulk single-phase channel flow. The latter approach risks over-simplifying the input features, but may lead to models that are more generalizable and easier to train across a wider dataset.

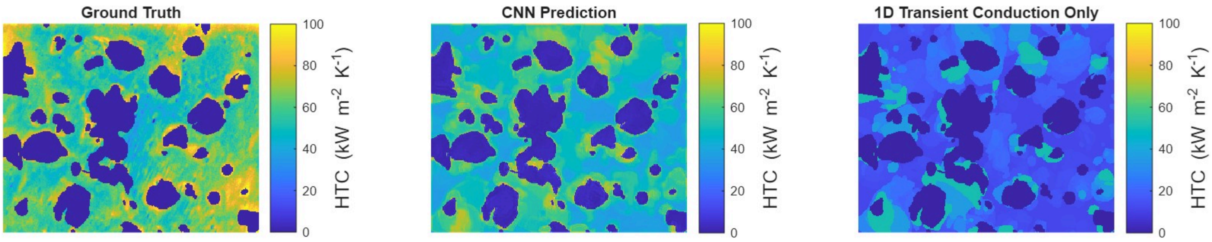

Figure 5. Sample results of the experimentally measured liquid HTC (left), predictions from our CNN model (middle), compared against the original 1D mechanistic reconstruction (right).

5. Conclusions

In this work, we developed a model to reconstruct the single-phase liquid heat transfer coefficient from optical data alone. This was achieved by developing a CNN model using pre-processed forms optical imaging. One input feature included the instantaneous near-wall velocity field inferred from our phase detection images, and the other input feature was the 1D transient conduction liquid HTC field using a simple reconstruction of the phase detection images. The combination of these two features resulted in a systematic increase in the steady-state HTC and transient HTC for a fixed wet time. We discuss some current limitations of this approach and recommendations that will establish a pathway for extracting near-wall transport information from optical data alone, providing guidance for future measurement and preprocessing strategies.

6. Acknowledgments

Matteo Bucci gratefully acknowledges the financial support of the Office of Naval Research (MURI N00014-24-1-2575), with Dr. Mark Spector serving as the program officer.

7. References

[1] N. Kurul, M.Z. Podowski, Multidimensional Effects in Forced Convection Subcooled Boiling, in: Begel House Inc., 1990. https://doi.org/10.1615/IHTC9.40.

[2] A. Richenderfer, A. Kossolapov, J.H. Seong, G. Saccone, E. Demarly, R. Kommajosyula, E. Baglietto, J. Buongiorno, M. Bucci, Investigation of subcooled flow boiling and CHF using high-resolution diagnostics, Exp. Therm. Fluid Sci. 99 (2018) 35–58. https://doi.org/10.1016/j.expthermflusci.2018.07.017.

[3] G.M. Aguiar, Infrared Thermometry Analysis of Surface Effects in Subcooled and Saturated Boiling of Water, Massachusetts Institute of Technology, 2024.

[4] G.M. Aguiar, M.T. Hughes, M. Bucci, On the nature of single-phase liquid heat transfer mechanisms in nucleate boiling: Evidence from high-resolution diagnostics, Int. J. Multiph. Flow 198 (2026) 105622. https://doi.org/10.1016/j.ijmultiphaseflow.2026.105622.

[5] A. Kossolapov, B. Phillips, M. Bucci, Can LED lights replace lasers for detailed investigations of boiling phenomena?, Int. J. Multiph. Flow 135 (2021) 103522. https://doi.org/10.1016/j.ijmultiphaseflow.2020.103522.

[6] M. Bucci, A. Richenderfer, G.-Y. Su, T. McKrell, J. Buongiorno, A mechanistic IR calibration technique for boiling heat transfer investigations, Int. J. Multiph. Flow 83 (2016) 115–127. https://doi.org/10.1016/j.ijmultiphaseflow.2016.03.007.